Optimization of High Temperature Hoop Creep Response in ODS-Fe_3Al Tubes

Bimal K. Kad[1], James H. Heatherington[1]
[1]University of California - San Diego, La Jolla, CA 92093
Claudette McKamey[2], Ian Wright[2], Vinod Sikka[2] and Rod Judkins[2]
[2]Oak Ridge National Laboratory, Oak Ridge, TN 37830

ABSTRACT

Oxide dispersion strengthened (ODS) Fe_3Al alloys are currently being developed for heat-exchanger tubes for eventual use at operating temperatures of up to 1100°C in the power generation industry. The development challenges include a) efforts to produce thin walled ODS-Fe_3Al tubes, employing powder extrusion methodologies, with b) adequate increased strength for service at operating temperatures to c) mitigate creep failures by enhancing the as-processed grain size. A detailed and comprehensive research and development methodology is prescribed to produce ODS-Fe_3Al thin walled tubes. Current single step extrusion consolidation methodologies typically yield 8ft. lengths of 1-3/8" diameter, 1/8" wall thickness ODS-Fe_3Al tubes. The process parameters for such consolidation methodologies have been prescribed and evaluated as being routinely reproducible. Recrystallization treatments at 1200°C produce elongated grains (with their long axis parallel to the extrusion axis), typically 200-2000μm in diameter, and several millimeters long. The dispersion distribution is unaltered on a micro scale by recrystallization, but the high aspect ratio grain shape typically obtained limits grain spacing and consequently the hoop creep response. Improving hoop creep in ODS-alloys requires an understanding and manipulating the factors that control grain alignment and recrystallization behavior. Current efforts are focused on examining the processing dependent longitudinal vs. transverse creep anisotropy, and exploring post-extrusion methods to improve hoop creep response in ODS-Fe_3Al alloy tubes. In this report we examine the mechanisms of hoop creep failure and describe our efforts to improve creep performance via variations in thermal-mechanical treatments.

Research Sponsored by the U.S. Department of Energy, Office of Fossil Energy, Advanced Research Materials Program, under contract DE-ACOR-96OR22464 with UT-Batelle subcontract to the University of California-San Diego.

Introduction

Oxide dispersion strengthened ferritic FeCrAl (MA956, PM2000, ODM751) and the intermetallic Fe_3Al-based alloys are promising materials for high temperature, high pressure, tubing applications, due to their superior corrosion resistance in oxidizing, oxidizing/ sulphidizing, sulphidizing, and oxidizing/chlorinating environments[1-4]. Such high temperature corroding environments are nominally present in the coal or gas fired boilers and turbines in use in the power generation industry. Currently, hot or warm working of as-cast ingots by rolling, forging or extrusion in the 650-1150^oC temperature range is being pursued to produce rod, wire, sheet and tube products[5-7]. *A particular 'in service application' anomaly of ferritic and* Fe_3Al*-based alloys is that the environmental resistance is maintained up to 1200*^oC*, well beyond where such alloys retain sufficient mechanical strength.* Thus, powder metallurgy routes, incorporating oxide dispersions, are required to provide adequate strength at the higher service temperatures.

The target applications for ODS-Fe_3Al base alloys in the power generation industry are thin walled (0.1" thick) tubes, about 1 to 3 inches in diameter, intended to sustain internal pressures (P) of up to 1000psi at service temperatures of 1000-1100^oC. Within the framework of this intended target application, the development of suitable materials containing Y_2O_3 oxide dispersoids must strive to deliver a combination of high mechanical strength at temperature, as well as prolonged creep-life (hoop creep in particular) in service. Such design requirements are at odds with each other, as strengthening measures severely limit the as-processed grain size, resulting in decreased creep life. Thus post-deformation recrystallization processes are essential to increase the grain size, and possibly modify the grain shape for the anticipated use. This paper describes our microstructure and property optimization of ODS-Fe_3Al alloy tubes, with a view to improving the high temperature creep response. In particular, we examine thermal-mechanical processing steps to affect and enhance secondary recrystallization kinetics and abnormal grain growth during post-extrusion processing to create large grains. Such procedures are particularly targeted to improve hoop creep performance at service temperatures and pressure.

Experimental Details

Three separate powder batches (labeled as A, B, C) of the Fe_3Al+0.5wt%Y_2O_3 composition were milled. Table 1 lists the alloy powder chemistry before and after three separate milling conditions[9]. Two separate analyses (labeled as HM, PM) were performed for the starting powders as listed in the table. The powders are labeled as A, B and C in the order of decreasing total interstitial (C+N+O) impurity. Process control agents were used for all milled batches and batch C was milled for a short period. As shown later this interstitial impurity plays a crucial role in the recrystallization kinetics and the resulting microstructures. The milled powders were encapsulated and vacuum-sealed in annular cans at

Figure 1. Assorted ODS-Fe_3Al alloy tubes in the as extruded and surface finished condition produced via an annular can (top left) consolidation methodology.

about 400°C. Sealed cans were then soaked over the 1000-1100°C temperature range for 2 hours and directly extruded into tubes via the single step extrusion consolidation over a mandrel. Figure 1 shows a set of tubes in the as extruded and surface finished condition. Further extrusion processing parameters are available elsewhere[7,8]. The tubes (6-8 ft. long, 1-3/8" diameter, 1/8" wall thickness) are of sound quality and exhibit no cracking after routine machining operations.

Table 1: Chemical analyses of the as-received and milled powder batches[9]

Element	As-Received HM	As-Received PM	Batch A	Batch B	Batch C
Fe	Bal.	79.6			
Al	16.3	18.20			
Cr	2.4	2.18			
Zr	20 ppm	26 ppm			
O (total)	60 ppm	110 ppm	1800 *ppm*	1900 *ppm*	1400 ppm
O (in Y_2O_3)			1025 *ppm*	1053 *ppm*	1080 ppm
O balance			775 *ppm*	847 *ppm*	320 ppm
O *pickup*			**665 *ppm***	**737 *ppm***	**210 ppm**
N	18 ppm	7 ppm	1264 *ppm*	145 *ppm*	88 *ppm*
N *pickup*			**1257 *ppm***	**138 *ppm***	**81 *ppm***
C		24 ppm	667 *ppm*	360 *ppm*	303 *ppm*
C *pickup*			**643 *ppm***	**336 *ppm***	**279 *ppm***
H		16 ppm	115 *ppm*	40 *ppm*	29 *ppm*
C+N+O *pickup*			**2565 *ppm***	**1211 *ppm***	**570 *ppm***

(Bulk compositions are identified in wt%) HM and PM are two separate analyses of atomized Fe_3Al powder

Recrystallization heat treatments were performed on short segments of the extruded tubes in the 1000-1300°C temperature range in air. Microstructures were examined using optical, SEM and TEM techniques. High temperature mechanical testing was performed on ASTM E-8 miniature samples extracted from the longitudinal and transverse orientations of the tubes. All further testing details are described in the relevant sections below.

Recrystallization Kinetics and Grain Structure

Recrystallization kinetics is affected both by extrusion ratio and the impurity levels in the milled powder batches. Initial recrystallization treatments were performed on powder consolidations performed at a 9:1 extrusion ratio, which proved very difficult to recrystallize[9]. A marked improvement in recrystallization kinetics is observed with the increased extrusion ratios, Figure 2. In essence, primary recrystallization can be initiated (but not necessarily completed) in all tubes extruded at ratios of 16:1 and higher[7,8]. The nominal recrystallization treatment is a 1hr soak at 1200°C in air. No recrystallization activity is observed at temperatures below 1100˚C in as-extruded tubes.

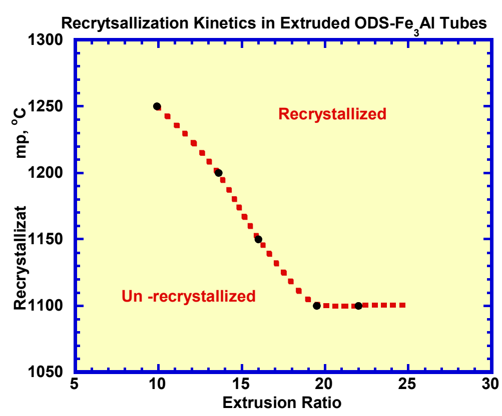

Figure 2. Recrystallization kinetics in the ODS-Fe_3Al tube extrusions.

Materials Characterization

Figure 3 shows the optical micrographs of polished and etched transverse section microstructures for the A (top) and the C (bottom) chemistry. We note that for tubes of batch A chemistry, Figure 3a, only a 25% section of the wall thickness (in the interior) exhibits primary recrystallization. As shown later via transmission electron microscopy studies, this primary recrystallized grain size remains small of the order of 1-2μm. However, tubes of batch C chemistry, Figure 3b, exhibit secondary recrystallization over the entire tube wall section in a reproducible manner. The recrystallized grains are elongated (with their long axis parallel to the extrusion axis), typically 200-2000μm in diameter, and several millimeters long. Additional aggressive thermal treatments (either reheating to higher temperature or prolonging the hold time) failed to initiate secondary recrystallization in the higher impurity (batch A, B) alloys.

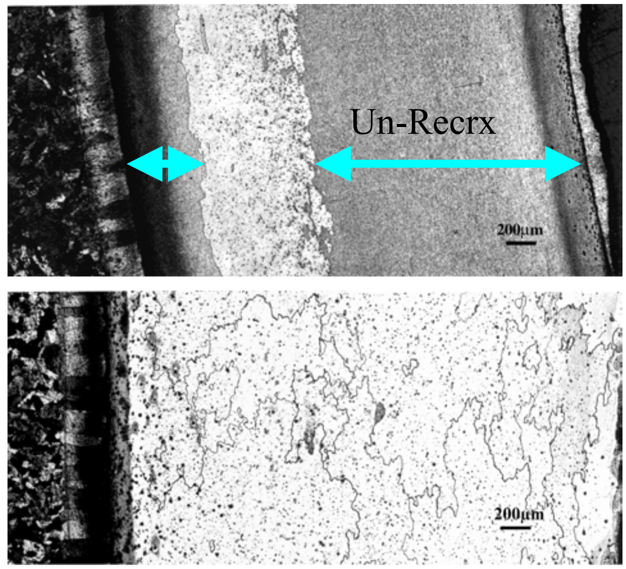

Figure 3. Recrystallized tube sections of (a) batch A (top) and (b) batch C (bottom) alloys.

TEM Microstructures

Bright field TEM micrographs of specimens extracted from the heat-treated tubes are shown in Figure 4. The 3mm diameter TEM discs are extracted from the wall thickness of the tubing such that foil normal and the extrusion axis are co-incident. With the TEM thin foil perforation

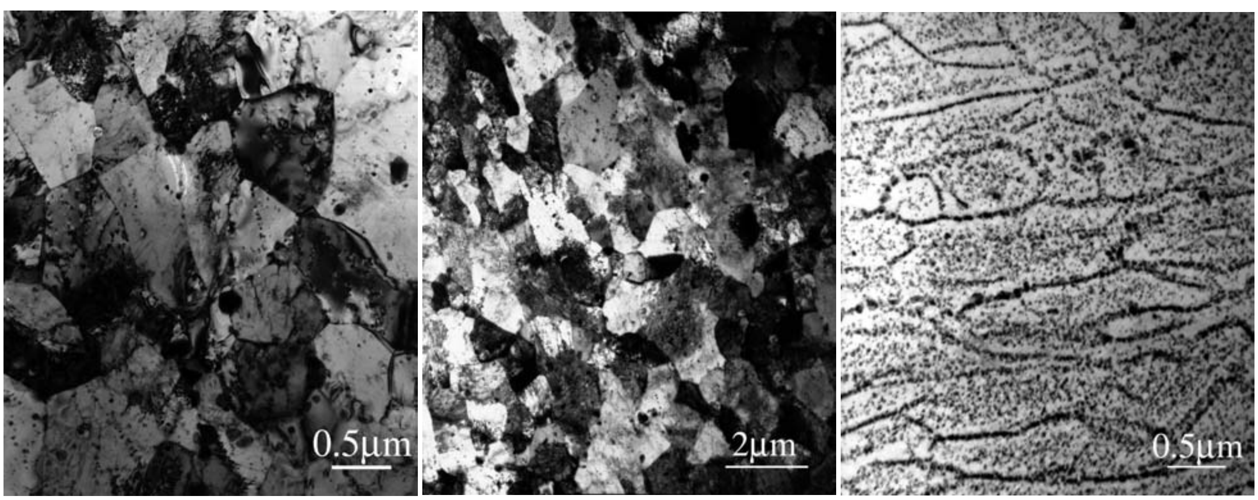

Figure 4. TEM micrographs of a) batch A, b) batch B and c) batch C specimens extracted from the heat-treated tubes. The viewing direction is along the extrusion axis. Batch A and B alloys exhibit the deformation processed and unrecrystallized {110} texture while batch C exhibits the recrystallized {111} texture.

expected near the center of the discs, the microstructures shown below are then representative of the center of the tube-wall thickness. The high impurity alloys (batch A and B) exhibit a fine-grained structure, Figure 4a, 4b with a {110} texture[10,11]. However, batch C exhibits a coarse grain structure with a {111} recrystallized texture[10], Figure 4c. The precipitate distribution in batch C is rather uniform but also exhibits a cell-type structure on the scale of 1 μm. This cell dimension is consistent with the as-extruded grain size and it is suggested that this particle distribution is originally present on the surface of the milled powders and upon consolidation is incorporated at the as-extruded grain boundaries. The Y_2O_3 precipitates are about 10-20nm in diameter and their distribution in batch C alloys is extremely homogenous at about 80-90nm spacing. This intra-granular dispersion distribution is separate from the milling induced impurity that coats the prior particle boundaries. The extent of such impurity pickup is milling process-dependent.

A magnified view of the batch B sample, Figure 5, illustrates that the grains are effectively pinned by precipitate particles. These precipitates (marked by red arrows) tend to be of the order of 0.25μm, i.e. much larger than the mean Y_2O_3 intra-granular dispersions of about 10nm size. Precipitate chemical analyses confirm that they contain negligible amounts of yttrium and instead are rich in aluminum. This is reflected in the relative strengths of the aluminum peak in the matrix and precipitate spectra as illustrated in Figure 5. Looking back to the interstitial impurity analysis of Table 1, we note that both batch A and B have a significant level of oxygen, nitrogen pickup depending on the exact milling conditions employed. This impurity is in addition to the oxygen in Y_2O_3 and is interpreted as an overall increase in the precipitate volume fraction via the formation of aluminum oxide and/or aluminum nitride at the prior particle surface.

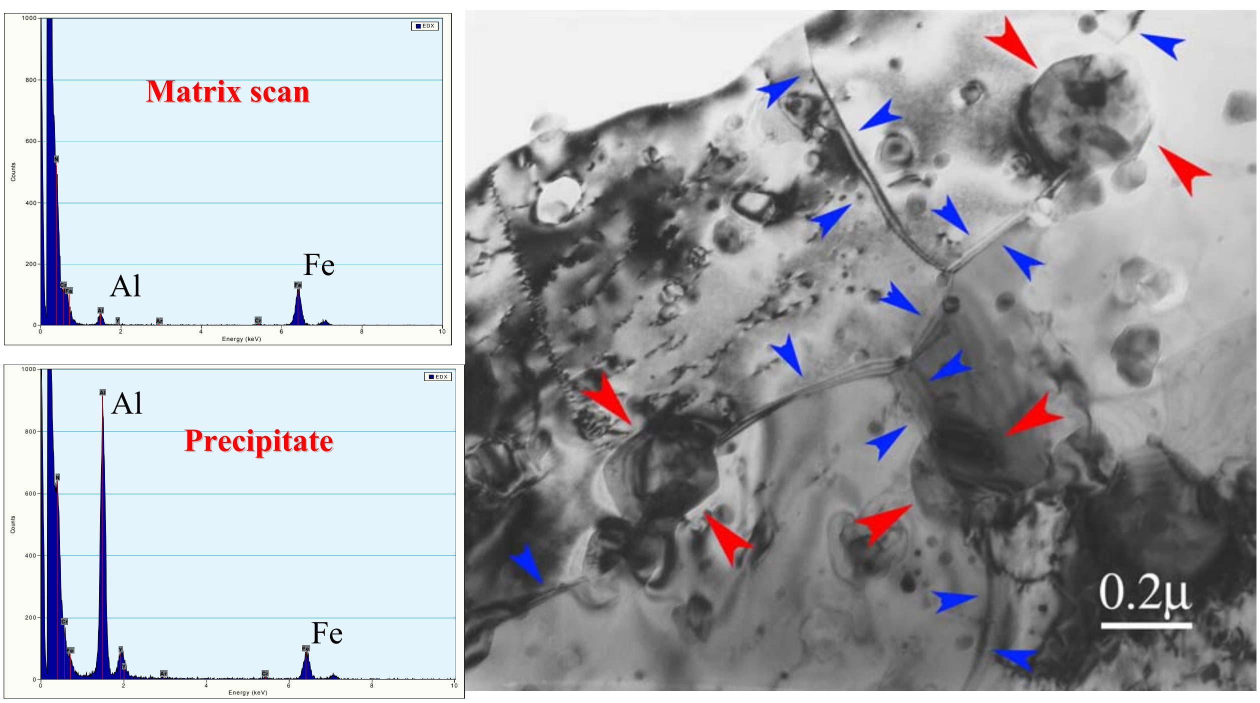

Figure 5. Impurity pickup at the milling stage results in the formation of large oxides and/ or nitrides of aluminum at the grain boundaries. Note: Blue arrows denote grain boundary and red arrows denote particles. All particles are aluminum-rich.

High Temperature Creep Properties

High temperature creep testing is limited to the 800 - 1100°C range (i.e., in the creep regime) for all the three tubes. Standard ASTM E-8 miniature specimens are extracted from tube sections for creep tests in the longitudinal and transverse orientations. Longitudinal sections are spark machined directly from tubes and transverse sections are machined from flattened (hot pressed at 900°C) tubes. The hot pressing temperature is limited to 900°C to prevent any recrystallization at this step. Samples are initially heat-treated at 1200°C for 1 hour.

Longitudinal vs. Transverse Creep Anisotropy

Preliminary creep tests were carried out for the ODS-Fe_3Al as well as the commercially available MA956 alloy tubes. The Fe_3Al samples were subjected to a uniform recrystallization heat treatment at 1200°C for 1 hour. Commercial MA956 tubes were recrystallized at 1350°C for 1 hour. Figure 6 shows the longitudinal (L) vs. transverse (T) creep anisotropy for both the Fe_3Al and the commercial MA956 (FeCrAl) alloys. The ODS-Fe_3Al tests were conducted at 1000°C in air and the MA956 test were conducted in the 900-1000°C temperature range in air. We note the improved creep response (see black arrows) of the Fe_3Al batch C chemistry over the commercial MA956 alloy in both the L and T orientations. The longitudinal and transverse creep response of ODS-Fe_3Al powder batches A and B (not shown here) is much inferior to that of batch C. This poor performance stems directly from the milling induced impurities that inhibit primary and secondary recrystallization. Thus, batch C is selected as the most promising alloy chemistry for further development based on the large recrystallized grain size and superior hoop creep responses.

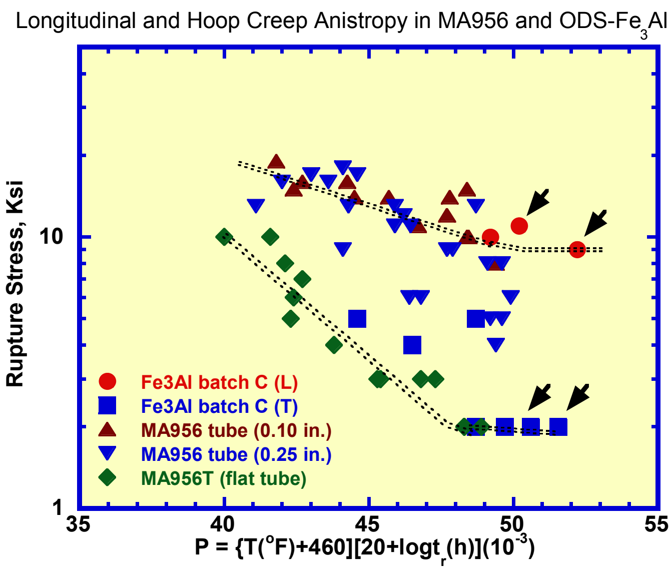

Figure 6. The longitudinal vs. transverse creep anisotropy for the ODS-Fe_3Al and MA956 alloys.

Transverse creep failures in ODS-Fe_3Al alloys

A mechanistic understanding of hoop creep failures is an important prerequisite to aid any subsequent microstructural modifications and/or redesign efforts at the system, sub-system or component level. Figure 7a shows a typical transverse creep failure as observed in fully recrystallized ODS-Fe_3Al alloy (batch C) tested at 1000°C. Significant ductile lobes and voids are observed and it is presumed that failure is preceded by void formation and coalescence. A better insight into the origin of voids is obtained by examining the specimen surface immediately below the creep failure. Figure 7b shows void formation in crept ODS-Fe_3Al and the origin of such voids is predominantly at the grain boundary. The tensile creep loading direction as indicated in Figure 7b is vertical. Similar results (not reported here) are also obtained for the MA956 transverse creep tests.

Our program efforts are directed towards exploring metallurgical and microstructural means to enhancing and optimizing hoop creep response. Presently variations in recrystallization heat-treatments and thermal-mechanical processing schemes are being explored for the ODS-Fe_3Al alloys. Table 2 lists the compiled results of various thermal recrystallization variations performed for batch C alloys and their ensuing creep response. In each case spark machined samples were heat-treated bare with or without a protective atmosphere. Samples are tested at a constant load and temperature and held for about 1000 hours at each stress level before incrementing the stress. The accumulated test time is recorded for the peak load and all prior load values. The observed creep rate is tabulated in days and L-M is the computed Larson Miller parameter. For example, Test #10 has 1325 hours of exposure at 2ksi and about 299 hours at the 3ksi increment (*i.e.* stress incremented after 1026 hours), and the creep rate is recorded as $4e^{-5}$/day at the 3ksi test condition. It is surmised that a 1000 hour exposure is sufficient for predicting long-term survivability at a specific test condition on account of the high stress exponent for failure. This is observed in such ODS-alloys particularly in the transverse orientation creep tests.

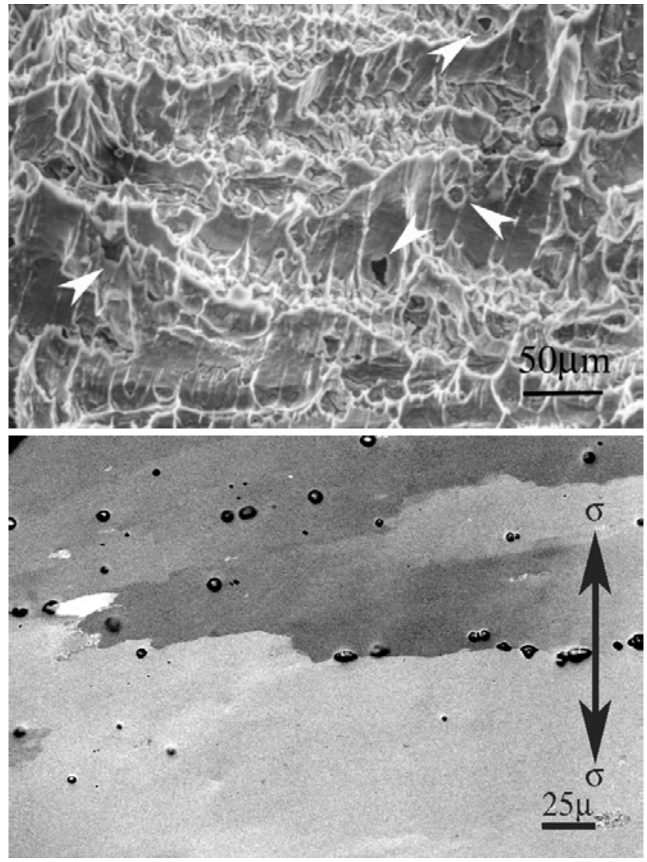

Figure 7. Transverse creep failure by void formation and coalescence in ODS-Fe_3Al crept at 3ksi at 1000°C. a) fracture surface (top) and b) specimen surface just below the fracture surface (bottom).

Table 2: Transverse creep response in ODS-Fe_3Al alloys as a function of thermal treatments.

Sample	Heat Treatment, Air	T°C	Ksi	Life	rate/day	L-M
#06, C2T	**1200°C/1hr+1300°C/1hr**	**900**	**2**	**643**	**$1.3e^{-3}$**	**48.17**
#20, C2T	**1300°C/1hr**	**900**	**2**	**2110**	**$7e^{-5}$**	**49.26**
#20, C2T	**1300°C/1hr**	**900**	**3**	**146**		**46.81**
#08, C2T	**1200C/1hr + 1250C/10hr**	**900**	**2**	**1093**		**48.66**
#08, C2T	**1200C/1hr + 1250C/10hr**	**900**	**3**	**90**	**$7e^{-4}$**	**46.37**
#05, C2T	**1250°C/10hr**	**1000**	**1**	**208**	**$1.6e^{-3}$**	**51.15**
#10, C2T	**1200°C/1hr**	**900**	**2**	**1325**		**48.83**
#10, C2T	**1200°C/1hr**	**900**	**3**	**299**	**$4e^{-5}$**	**47.47**
#15, C2T	**1200°C/1hr**	**1000**	**1**	**4315**	**$1e^{-4}$**	**54.17**

Aggressive recrystallization heat treatments

Figure 8 shows a direct comparison of creep response of high purity (batch C) alloys heat-treated at different temperatures in air. The exact data is from Test #6 and #10 (indicated in Table 2) as tested at 2ksi stress at 900°C. The 1300°C heat-treatment was conducted by re-heating a test sample previously recrystallized at 1200°C. A higher creep rate is observed for the 1300°C treatment. Another example is a direct comparison of test #5 and #15 where aggressive thermal exposure (for test #5) does not improve creep-life in ODS-Fe_3Al alloys. Repeated tests, Table 2, indicate that creep response deteriorates with increasing recrystallization treatment temperature.

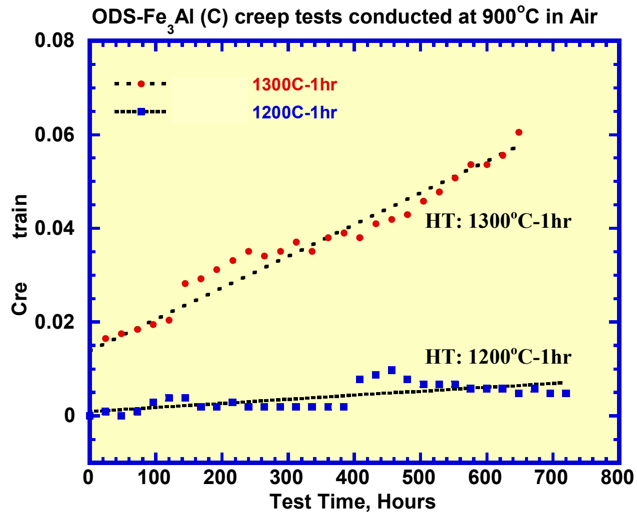

Figure 8. Comparison of creep rates and strain for different recrystallization heat-treatments.

Within the context of aggressive thermal treatments it is important to note that commercial ODS-FeCrAl alloys are recrystallized in the 1300-1400°C range. Looking back to Figure 6, we note the improved creep response (see arrows) of the Fe_3Al batch C chemistry over the commercial MA956 alloy in both the L and T orientations. This trend is consistent with the higher recrystallization temperatures employed for MA956 alloys. This aggressive temperature is in part necessary to overcome the Zener pinning as the Y_2O_3 dispersion volume fraction is about 15% higher in MA956 alloys. Prior studies[12,13] indicate the formation of subsurface voids when samples are exposed to aggressive environments, and it is surmised that similar effects might be operative here. This effect may be particularly detrimental to transverse creep response – which in fact fails via grain boundary void formation and coalescence. Efforts to decrease the recrystallization temperature in commercial ODS-ferritic and intermetallic Fe_3Al alloys may be a promising avenue of further ODS-alloy development.

Variations in thermal-mechanical processing

Thermal-mechanical processing efforts have been prompted by the extreme longitudinal vs. transverse (hoop) creep anisotropy in ODS-Fe_3Al and MA956 alloys, Figure 6. Clearly there are different mechanisms of creep failure at work in the orthogonal orientations. Longitudinal creep limit is dictated by ODS strengthening of the matrix while transverse creep strength is limited by the grain boundary void formation and coalescence, Figure 7. Such boundary void formation is further enhanced by the presence of large impurity oxides, Figure 5, and unrecrystallized stringers aligned along the primary extrusion axis (i.e., normal to the hoop loading axis). Thus the strength anisotropy is linked with the underlying grain structure of the processed tubes.

With respect to the end-use application of internally pressurized tubes, the hoop stress required is twice the longitudinal stress. This application specific requirement is at odds with (and inverse of) the intrinsic material anisotropy illustrated in Figure 6. What is clearly desired is an exploration of likely thermo-mechanical methodologies to alter the underlying grain structure. Such a process is routine in plates and sheets, which are cross-rolled to effect isotropic in-plane response. Cross rolling of tubes is a technical challenge and as a first step flattened tube segments (of as-extruded tubes) were cross-rolled at 900^{o}C in multiple passes to a total of 25% thickness reduction. Samples in the transverse orientation (to the original tube) were spark machined from the rolled plate and ground to remove the canned layer. They were further pre-oxidized at 900^{o}C for 30 minutes prior to the recrystallization heat-treatment of 1200^{o}C for 1 hour in air. Preliminary creep tests on cross-rolled samples exhibit an order of magnitude reduction in the minimum creep rate. Looking ahead to the schematic representation of Figure 9, we note corresponding improvements in peak stress and creep life that are indeed encouraging. No failures have been observed to date and consequently further microstructural insights are awaited. Further plans to perform recrystallization under inert atmospheres are underway and will be evaluated for hoop creep performance in the near future.

Summary and Conclusions

High temperature creep response in ODS-Fe_3Al tubes is reported for the longitudinal and transverse orientations. The kinetics of grain growth is affected by interstitial impurity content, which limit the extent of recrystallized regions observed in the tube wall. Consequently, the microstructure exhibiting the best creep response is one of high purity that undergoes complete primary and secondary recrystallization.

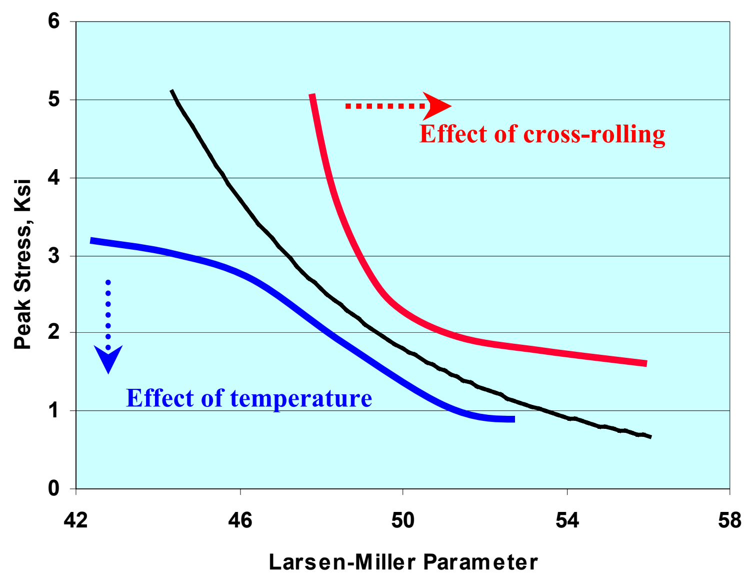

Figure 9. Processing dependent hoop creep response.

Figure 9 shows a schematic of the effect of various thermal-mechanical treatments on the ensuing hoop creep response in ODS-Fe_3Al alloys. The black curve is a median representation of all test results (not presented here) obtained to date. The blue curve indicates hoop creep response at aggressive thermal treatments where both peak stress bearing capacity and creep-life are diminished. The red curve is a partial construct of the beneficial effects of cross rolling aimed at altering the underlying grain structure. The results of optimization efforts to date are summarized as follows:

- Powder milling appears to be the most pervasive processing component dominating microstructural and material response. It is suggested that coarse nitrides and oxides of aluminum (formed during milling) inhibit recrystallization grain growth in high impurity alloys.

- Creep response of the respective powder batches is proportional to the underlying grain structure produced via heat-treatments. Thus, ODS Fe_3Al powder batch C with its completely recrystallized tube wall section offers the best creep response.

- Significant deterioration in hoop creep is observed in materials subjected to aggressive recrystallization temperatures. This observation is consistent with the improved performance of ODS-Fe_3Al alloys over MA956 alloys in equivalent tests performed in our laboratory.

- Thermo-mechanical processing to alter the underlying grain shape and structure has a directly beneficial effect on improving hoop creep response.

Acknowledgements

Electron microscopy studies were conducted in part at the DOE-BES funded SHaRE facility at the Oak Ridge National Laboratory with the assistance of Dr. Neal Evans and Dr. Jim Bentley.

References

1 C. Capdevila and H.K. Bhadeshia, 'Manufacturing and Microstructural Evolution of Mechanically Alloyed Oxide Dispersion Strengthened Superalloys', *Advanced Engineering Materials*, 2001, **3**(9), 647.
2. R.F. Singer and E. Arzt, *High Temperature Alloys for Gas Turbine and Other Applications*, D. Reidel Publishing Co., Liege, 1986.
3. F. Starr, 'Emerging Power Technologies and Oxide Scale Spallation', *Mater. High. Temp*., 1995, **13**(4), 185-192.
4 B.A. Pint and I.G. Wright, 'Long Term High Temperature Oxidation Behavior of ODS Ferritics', *Journal of Nuclear Materials*, 2002, **307-311**, 763-768.
5. V.K. Sikka, S. Viswanathan, C.G. McKamey, *Structural Intermetallics*, 1993, TMS Publication, Warrendale PA, 483.
6. P.G. Sanders, V.K. Sikka, C.R. Howell, R.H. Baldwin, 'A Processing Method to Reduce the Environmental Effect in Fe_3Al-Based Alloys', *Scripta Met*., 1991, **25**(10), 2365-2369.
7. B.K. Kad, 'Oxide Dispersion Strengthened Fe_3Al Bases Alloy Tubes', *Advanced Research Materials Report*, ORNL/Sub/97-SY009/02, October 2001.
8. B.K. Kad, V.K. Sikka and I.G. Wright, 'Oxide Dispersion Strengthened Fe_3Al-Based Alloy Tubes', *14th Ann. Conf. Fossil Energy Materials*, Knoxville, TN, May 2000; *ibid*. 'High Temperature Performance of ODS Fe_3Al-Based Alloy Tubes' *15th Ann. Conf. Fossil Energy Materials*, Knoxville, TN, April 2001.
9. I.G. Wright, B.A. Pint, E.K. Ohriner and P.F. Tortorelli, 'Development of ODS- Fe_3Al Alloys', *Proc. 11th Ann. Conf. on Fossil Energy Materials*, 1996, ORNL Report ORNL/FMP-96/1, CONF-9605167, p. 359.
10. B.K. Kad, S.E. Schoenfeld, R.J. Asaro, C.G. McKamey, V.K. Sikka, 'Deformation Textures in Fe_3Al Alloys: An Assessment of Dominant Slip System Activity in the 900-1325K Temperature Range of Hot Working', *Acta Metallurgica*, 1997, **45**(4), 1333-1350.
11. M. Mujahid, C.A. Carter and J.W. Martin, 'Microstructural Study of a Mechanically Alloyed ODS Superalloy', *J. Mater. Eng. Performance*, 1998, **7**(4), 524.
12. Y. Iino, 'Effects of High Temperature Air and Vacuum Exposure on Tensile Properties and Fracture of ODS Alloy MA6000', *Mater. Sci. Eng*., 1997, **A234-236**, 802-805.
13. A. Czyrska-Filemonowicz, D.Clemens and W.J. Quadakkers, 'The Effect of High Temperature Exposure on the Structure and Oxidation Behavior of Mechanically Alloyed Ferritic ODS Alloys', *J. of Mater. Proc. Tech*., 1995, **53**, 93-100.